

Communication

Removal of 2,4-Dichlorophenoxyacetic Acid from Aqueous Solutions Using Al₂O₃/Graphene Oxide Granules Prepared by Spray-Drying Method

Alexandra Yu. Kurmysheva ¹, Ekaterina Kuznetsova ^{2,*}, Marina D. Vedenyapina ³, Pavel Podrabinnik ¹, Nestor Washington Solís Pinargote ², Anton Smirnov ² and Sergey N. Grigoriev ¹

¹ Laboratory of Electric Current Assisted Sintering Technologies, Moscow State University of Technology “STANKIN”, Vadkovsky per. 1, 127055 Moscow, Russia; aukurm@gmail.com (A.Y.K.); p.podrabinnik@stankin.ru (P.P.); s.grigoriev@stankin.ru (S.N.G.)

² Laboratory of 3D Structural and Functional Engineering, Moscow State University of Technology “STANKIN”, Vadkovsky per. 1, 127055 Moscow, Russia; nw.solis@stankin.ru (N.W.S.P.); a.smirnov@stankin.ru (A.S.)

³ N. D. Zelinsky Institute of Organic Chemistry, Russian Academy of Sciences, Leninsky Prospect 47, 119991 Moscow, Russia; mvedenyapina@yandex.ru

* Correspondence: e.kuznetsova@stankin.ru

Abstract: Within this study, aluminum oxide granules with 0.25%vol. of graphene oxide were prepared by a spray-drying method to make an adsorbent for the 2,4-Dichlorophenoxyacetic acid (2,4-D) herbicide removal from aqueous solutions. The obtained adsorbent was studied using infrared spectroscopy, scanning electron microscopy and Raman spectroscopy. The presence of graphene in the spray-dried powder was confirmed. The adsorption removal of 2,4-D using the obtained material was performed at an ambient temperature by varying the process parameters such as pH and adsorption time. The adsorption of 2,4-D was a monolayer chemisorption according to the Langmuir isotherm pattern and a pseudo-second-order kinetic model. The maximum Langmuir adsorption capacity of the monolayer was 35.181 mg/g. The results show that the Al₂O₃-0.25%vol. GO powder obtained by spray drying is suitable for the production of adsorbents for toxic herbicides.

Keywords: 2,4-D adsorption; herbicide adsorption; alumina adsorbent; graphene oxide; spray dry



Citation: Kurmysheva, A.Y.; Kuznetsova, E.; Vedenyapina, M.D.; Podrabinnik, P.; Pinargote, N.W.S.; Smirnov, A.; Grigoriev, S.N. Removal of 2,4-Dichlorophenoxyacetic Acid from Aqueous Solutions Using Al₂O₃/Graphene Oxide Granules Prepared by Spray-Drying Method. *Resources* **2024**, *13*, 40. <https://doi.org/10.3390/resources13030040>

Academic Editor: Diego Copetti

Received: 19 January 2024

Revised: 23 February 2024

Accepted: 6 March 2024

Published: 11 March 2024



Copyright: © 2024 by the authors. Licensee MDPI, Basel, Switzerland. This article is an open access article distributed under the terms and conditions of the Creative Commons Attribution (CC BY) license (<https://creativecommons.org/licenses/by/4.0/>).

1. Introduction

Today, natural water reservoirs contain large amounts of pollutants as a result of human economic activities. Xenobiotic substances including pesticides and herbicides used in agriculture, e.g., 2,4-dichlorophenoxyacetic acid (2,4-D), contribute the most to that pollution. Being widespread and highly soluble, 2,4-D and its transformation products have polluted natural water and soil resources [1]. Moreover, 2,4-D was reported to stand behind the cancer-disease development in mammals, as well as endocrine and central nervous system disorders [2–4].

The method of adsorption extraction for pollutants from aqueous solutions is widely used for wastewater treatment thanks to the ease of the adsorber design, low cost, mild process conditions and the absence of harmful secondary products [5]. A large list of sorbents was already studied for the 2,4-D removal from aqueous solutions, including magnetically activated carbons [6], a metal-organic framework [7], polymer compounds [8] and graphene oxide aerogel [9].

Sorbents based on aluminum oxide (Al₂O₃) have been widely used in various fields of industry and medicine for a long time due to their beneficial properties [10]. The Al₂O₃ compound combines high mechanical strength, hardness, a developed surface and chemical resistance, while its cost is reasonably low [11,12]. Currently, special attention is paid to adsorbents with alumina, which exhibit very good adsorption properties towards

heavy metals [13,14]. In addition, being water-resistant, aluminum oxide is often used as an adsorbent for drying and processing media containing condensed moisture, while the possibility of repeated temperature regeneration by burning ensures the long-term operation of the adsorbent [15].

In recent years, much attention has been paid in the literature to graphene oxide (GO) as a promising adsorbent for organic pollutants due to the presence of oxygen-containing functional groups on its surface, which can act as adsorption centers [16]. However, two-dimensional GO has poor structural stability in aqueous environments, making it difficult to recover and reuse [9,17].

Adsorbents containing a single component often require a functionalization of their surface, such as, for example, increasing the specific surface area, creating additional micro and mesopores, and applying functional groups to improve the adsorption capacity in relation to target pollutants. Such functionalization can be achieved through the additional activation of the raw material, doping the sorbent with various substances [18], and also creating composites.

To enhance aluminum oxide, it was suggested to combine it with graphene oxide by spray drying to obtain a granulated Al_2O_3 -0.25%vol. GO adsorbent. The technique provides a spherical shape to the particles that contributes to the adsorption process. Spray drying makes it possible to obtain granules ranging in size from several to tens of microns from highly dispersed and ultra-disperse ceramic powders from solutions or suspensions by drying [19]. Compared to other methods for obtaining carbon nanomaterials such as milling, sintering and crushing, the spray granulation method avoids the agglomeration of GO nanosheets and reduces damage to their structure [20].

Thus, the purpose of this work was to obtain a new sorbent from aluminum oxide with the addition of 0.25% vol of GO and to study its adsorption ability for 2,4-D from aqueous solutions.

2. Materials and Methods

2.1. Materials

For the research, the following raw materials were obtained: 2,4-Dichlorophenoxyacetic acid (Merck, Darmstadt, Germany), NaOH ($\geq 99\%$), NaCl ($\geq 99\%$), HCl (37%) (Khimprom, Kemerovo, Russia), α - Al_2O_3 powder with purity 98.9–99.9% and average particle size of 500 nm (Plasmotherm Ltd., Moscow, Russia), polyvinyl alcohol (Ruskhim Ltd., Moscow, Russia) and aqueous suspension of GO with a concentration of 50 mg/mL (Graphenox, Moscow, Russia).

2.2. Adsorbent Preparation

The Al_2O_3 -0.25GO sorbent was produced by spray drying from a prepared suspension for granulation. To obtain a suspension, at the first stage, graphene oxide was dispersed in distilled water with a concentration of 0.6 mg/L by the IKA T-18 (IKA-Werke GmbH & Co. KG, Staufen, Germany) ultrasound homogenizer. Next, aluminum oxide and a dispersant (0.01 wt.% Al_2O_3) were added to the suspension to prevent the sticking of Al_2O_3 particles and the formation of large agglomerates. Then, the suspension was placed on a MR Hei-Tec (Heidolph Instruments GmbH & Co. KG, Schwabach, Germany) magnetic stirrer, and a solution of polyvinyl alcohol (0.2% wt.) was added as a binder. The composition was mixed for 6 h at a speed of 400 rpm/min. To demonstrate the effect of graphene oxide on the adsorption properties of the composite, aluminum oxide powder was obtained in a similar way without the addition of graphene oxide (Al_2O_3 -0GO).

2.3. Characterization of Adsorbent

Microstructural analysis was performed using scanning electron microscope Vega 3 LMH (SEM, Tescan, Brno, Czech Republic). In order to avoid electron charging and improved imaging, samples were coated by electrically conductive thin gold film using Q150T Emscope (Quorum Technologies Ltd., Newhaven, UK) sputter coater. Raman

spectroscopy of the produced samples was carried out using DXR™2 microscope (Thermo Fisher Scientific, Waltham, MA, USA) equipped with a 780 nm laser with a power of 15 mW. The laser beam was to pass through 50× optical zoom lens projecting into 0.8 μm spot on the examined area with an integration time of about 6 s for each spectrum. Fourier transform infrared spectroscopy (FTIR) spectra were recorded using Vertex 70 (Bruker Optik GmbH, Ettlingen, Germany) spectrometer. To calculate the specific surface area S_{BET} , m²/g for the Al₂O₃-0.25GO specimen, a Brunauer–Emmett–Teller (BET) analysis was performed using Autosorb iQ Station 2 gas sorption analyzer (Quantachrome Instruments, Boynton Beach, FL, USA). The point of zero charge (pHzpc) of the adsorbent resulted from the pH drift method, described in [21], using S 210 pH meter (Mettler-Toledo, Columbus, OH, USA).

2.4. Adsorption

The adsorption of 2,4-D from aqueous solutions onto Al₂O₃-0.25GO and Al₂O₃ was carried out in thermostatic cells at a temperature of 25 °C with continuous mixing. To study the kinetics of adsorption, equal portions of the adsorbent weighing 25 mg were added to 100 mL of 2,4-D solution with concentrations of 10–200 mg/L. During the experiment, samples were taken from prepared adsorbate solutions with added adsorbent at specified time intervals. Adsorbate concentration in samples was determined using UV spectroscopy at 283 nm on a Hitachi U-1900 instrument (Tokyo, Japan). The number of ions of 2,4-D adsorbed per 1 g of the adsorbent (mg/g) was calculated according to Equation (1) below:

$$q_e = \frac{(C_0 - C_e) \cdot V}{m}, \quad (1)$$

where C_0 and C_e —initial and equilibrium concentration of each adsorbate ion, respectively; mg/L; V —volume of the solution, l; m —the mass of the adsorbent, g.

Preliminary experiments showed an insignificant adsorption ability of Al₂O₃-0GO. Thus, the calculation of the isotherms and kinetics of the adsorption process on aluminum oxide powder without the addition of graphene oxide was not considered in this work. All adsorption experiments were performed in triplicate, with the average values used for calculations.

3. Results and Discussion

3.1. Characterization of the Adsorbent

The calculated specific surface area of the sorbent was 6.852 m²/g, the total pore volume—0.043 cm³/g and the average pore diameter—25.32 nm. The microstructure of the sorbent is shown in Figure 1. The particles were almost spherical, with sizes ranging from 1 μm to 20 μm (Figure 1A). A microporous structure and a developed surface were also observed (Figure 1B).

Since the low content of GO in granules makes it hard to detect using SEM, it was identified using Raman spectroscopy. The Raman spectrum of the sorbent is given in Figure 2.

The results show that the spectrum has pronounced peaks of D and G bands with wave numbers of 1312 cm⁻¹ and 1592 cm⁻¹, respectively, which is typical for GO. This pattern is also common for carbon-containing materials. The G band is attributed to a perfect graphite structure while the D band shows defects in the microstructure. Therefore, after the spray drying, the sorbent retained the GO structure, which is consistent with the literature [22–24].

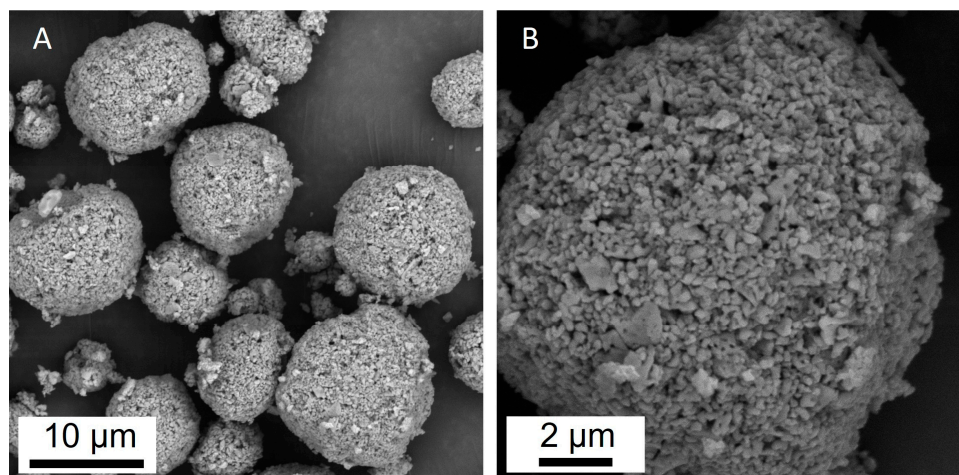


Figure 1. SEM images of the Al_2O_3 -0.25GO sorbent granules; (A) general view of the granules at magnification $\times 10,000$ and one granule at magnification $\times 30,000$ (B).

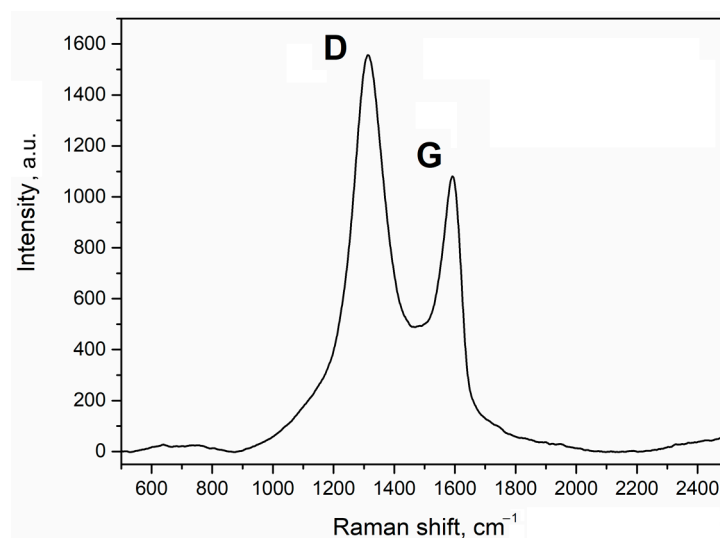


Figure 2. Raman spectrum of the Al_2O_3 -0.25GO sorbent granules.

Figure 3 shows the FTIR spectra of the Al_2O_3 -0GO and the Al_2O_3 -0.25GO specimens. Strong absorption bands at 600 cm^{-1} and 447 cm^{-1} can be attributed to stretching vibrations of the Al-O bond [25]. The Al_2O_3 -0.25GO specimen demonstrates characteristic bands 1215 cm^{-1} and 1280 cm^{-1} , confirming the presence of C-O-C bonds and the C-O stretching of an epoxy group [26]. The 1660 cm^{-1} peak can be identified as the in-plane vibrations of the skeletal C=C band of the hexagonal aromatic ring from the graphene sheet [25]. The peak at 3406 cm^{-1} is connected to the OH stretching of carboxylic groups. The characteristic band at 1760 cm^{-1} can be associated with the C-O stretching of the carboxylic group [26].

3.2. Adsorption Studies

3.2.1. Effect of pH

The pH of the solution is one of the most important parameters influencing the process of interaction of the adsorbate with the adsorbent. When the pH changed in the range from 2 to 10, the interaction between 2,4-D and the adsorbent also changed. The pH_{PZC} value was determined to characterize the surface charge of the adsorbent. It describes the electrically neutral environment of the sorbent surface at a certain pH of the solution. For an adsorbent, pH_{PZC} was found to be 7.6, which means that the total surface charge of the adsorbent will be positive at $\text{pH} > 7.6$ and negative at $\text{pH} < 7.6$. 2,4-D is a weak acid and is present in solution mostly in its anionic form. Based on pH_{PZC} data and the

resulting dependence presented in Figure 4, it is shown that the pH region most effective for adsorption is in the range of values from 2 to 4.

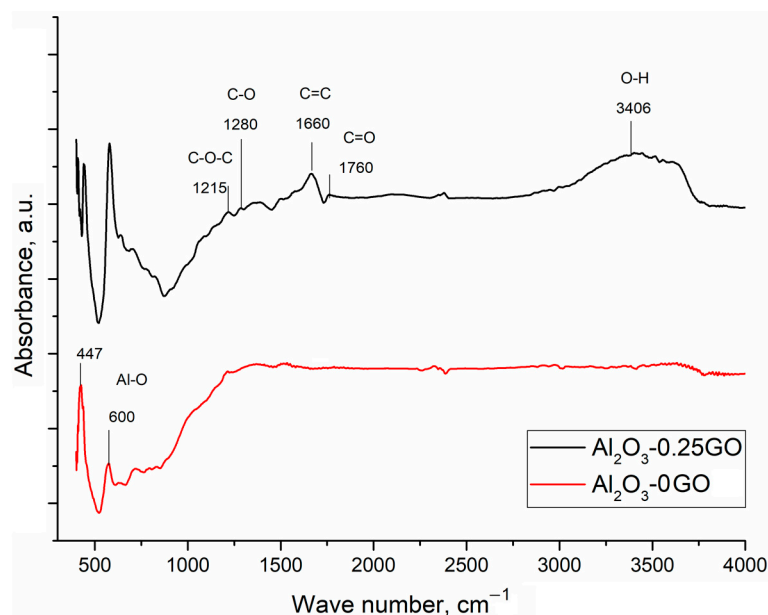


Figure 3. FTIR spectra of $\text{Al}_2\text{O}_3\text{-0GO}$ and $\text{Al}_2\text{O}_3\text{-0.25GO}$.

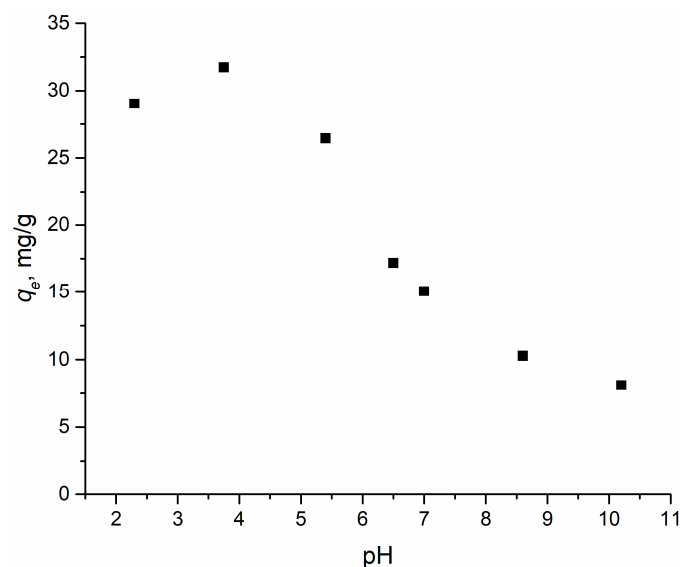


Figure 4. Effect of pH on the adsorption of 2,4-D using adsorbent. Points—the value of the experimental adsorption capacity, mg/g, at different pH values.

The obtained correlation and the pH_{PZC} concept suggest that electrostatic interactions are one of the main adsorption mechanisms of 2,4-D on that sorbent. However, a small adsorption capacity of $\text{Al}_2\text{O}_3\text{-0.25GO}$ to 2,4-D was observed in an environment with a pH higher than the pH_{PZC} value, which may be due to interactions such as π - π stacking between the aromatic rings of 2,4-D and GO or hydrogen interactions with oxygen-containing groups on the surface of the sorbent.

3.2.2. Adsorption Kinetics

Adsorption kinetics were evaluated by applying nonlinear pseudo-first-order (PFO) [27], pseudo-second-order (PSO) [28] and Elovich [29] kinetic models. The models are usually

taken to evaluate rate constants and adsorption rates. The kinetic parameters of the nonlinear PFO and PSO models were calculated using Equations (2) and (3), respectively:

$$q_t = q_e \cdot (1 - \exp^{-k_1 \cdot t}), \quad (2)$$

$$q_t = \frac{q_e^2 \cdot k_2 \cdot t}{1 + q_e^2 \cdot k_2 \cdot t}, \quad (3)$$

where k_1 (min^{-1}) and k_2 ($\text{g}/(\text{mg} \cdot \text{min})$) are the rate constants for PFO and PSO, respectively, and q_e and q_t (mg/g) are the number of adsorbed ions of 2,4-D at equilibrium and at time t , respectively.

The Elovich model is expressed in the following way (4):

$$q_t = \frac{1}{\beta} \ln(\alpha \beta t + 1), \quad (4)$$

where α ($\text{mg}/\text{g} \cdot \text{min}$)—initial adsorption rate; β (g/mg)—desorption constant during each experiment.

Figure 5 shows the results of the nonlinear models of a pseudo-first-order, pseudo-second-order and the Elovich kinetic model for the adsorption of 2,4-D on Al_2O_3 -0.25GO, and Table 1 contains the variables of the kinetic models.

Table 1. Kinetic models for the removal of 2,4-D.

C_0 , mg/L	Pseudo-First-Order			Pseudo-Second-Order			Elovich		
	k_1	q_{e1} , mg/g	R^2	k_2	q_{e2} , mg/g	R^2	α , mg/(g·min)	β , g/mg	R^2
25	0.023	25.19	0.989	0.001	28.914	0.998	1.84	0.15	0.988
50	0.026	28.189	0.993	0.001	32.173	0.999	2.393	0.15	0.982
75	0.027	30.092	0.993	0.001	34.21	0.999	2.787	0.15	0.982
100	0.036	30.622	0.984	0.002	33.888	0.999	6.89	0.18	0.988

The best fit to the kinetic model of 2,4-D adsorption on Al_2O_3 -0.25GO was shown using the PSO model ($R^2 > 0.99$). This indicates that the adsorption-limiting step involves inter- and intramolecular interactions between 2,4-D and the adsorbent. In this case, the rate of filling the adsorption centers on the Al_2O_3 -0.25GO surface is proportional to the number of unoccupied centers [30]. Although the Elovich kinetic model correlated less with experimental 2,4-D adsorption data, the β variable could be used to confirm the occurrence of inter or intramolecular interactions between the adsorbate and the adsorbent. The Elovich model assumes that real solid surfaces are energetically inhomogeneous, while the desorption process and the interaction between the adsorbed particles do not have a significant effect on the adsorption kinetics at low surface coverage. The α and β coefficients of the model represent the initial adsorption rate ($\text{mg}/(\text{g} \cdot \text{min})$) and the desorption coefficient (g/mg), respectively. The α coefficient was >1 $\text{mg}/(\text{g} \cdot \text{min})$ over the entire concentration range, while the β coefficient varied from 0.15 to 0.18 g/mg . This indicates a low desorption rate due to the effective interaction of 2,4-D and Al_2O_3 -0.25GO [31].

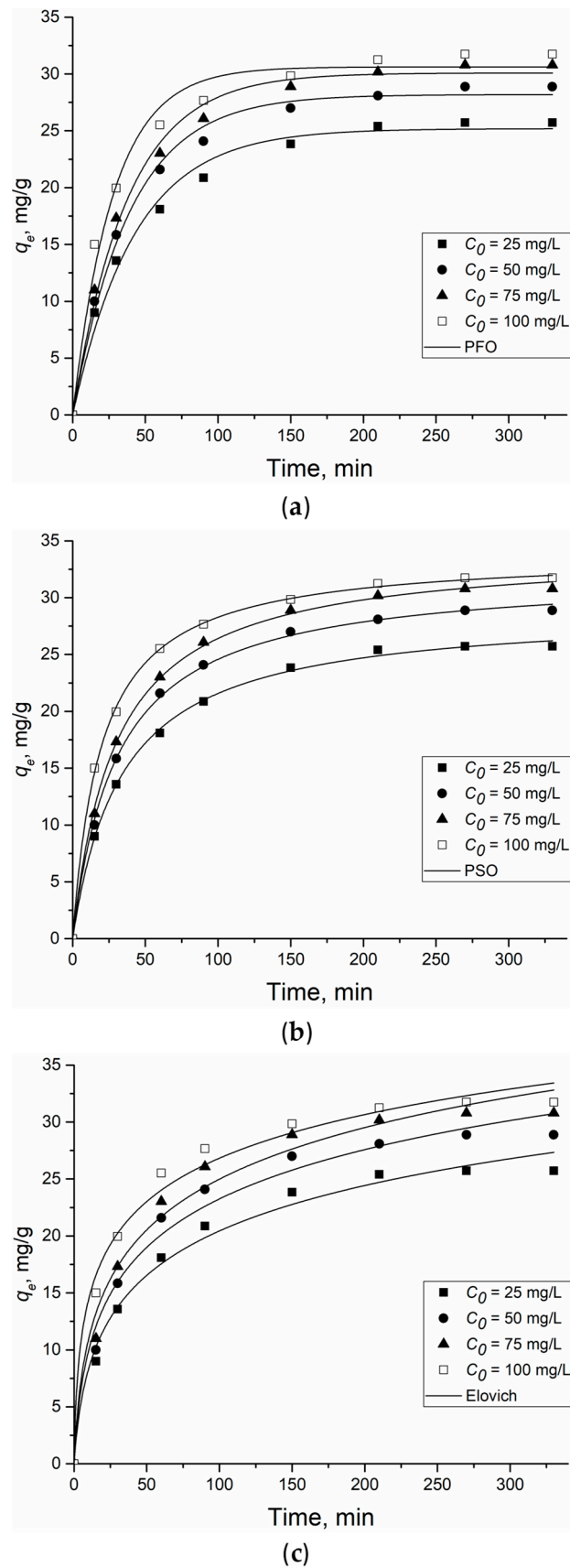


Figure 5. Pseudo-first-(a), pseudo-second (b)-order and Elovich (c) kinetic model of 2,4-D adsorption onto $\text{Al}_2\text{O}_3\text{-0.25GO}$. Dots are experimentally obtained data for various C_0 , lines—results of model calculations.

3.2.3. Adsorption Isotherms

The three widely used models of Langmuir [32], Freundlich [33] and Temkin [34] were used to describe the adsorption isotherms of 2,4-D on Al₂O₃-0.25GO. The simulation of adsorption isotherms provides insight into the interaction of the solute with the adsorbent and the nature of the adsorption process. These models show the dispersion behavior of the adsorbed fragments in the aqueous and solid phases when adsorption reaches equilibrium.

The nonlinear form of the Langmuir isotherm could be represented by Formula (5):

$$q_e = q_m b_L c_e / (1 + b_L c_e), \quad (5)$$

where q_m —maximum capacity of the monolayer (mg/g), and b_L —the adsorption coefficient (L/g). The Langmuir model assumes a single-layer coating of 2,4-D on the surface of the adsorbent.

According to Freundlich's theory, at a constant temperature, the amount of adsorbed solute per unit mass of the adsorbent is proportional to the equilibrium concentration of the substance adsorbed from the solution, raised to a certain power that is less than their unity. Mathematically, the Freundlich isotherm can be presented as in Equation (6):

$$q_e = K_F c_e^{1/n}, \quad (6)$$

where K_F —the coefficient of distribution or adsorption coefficient (L/g).

The Temkin isotherm model takes into account the adsorbate–adsorbent interaction and assumes that the heat of the adsorption of all the molecules in the layer will decrease linearly as adsorbed molecules accumulate on the surface of the adsorbent [35]. The isotherm was calculated according to Equation (7).

$$q_e = (RT/b_T) \ln(Ac_e), \quad (7)$$

where b_T —the adsorption coefficient (J/mole); R —the universal gas constant of 8.314 J/(mol·K); A —the constant, L/g; T —the absolute temperature (K).

Figure 6 shows the results of applying the isotherm models to the experimental data of the adsorption 2,4-D on Al₂O₃-0.25GO.

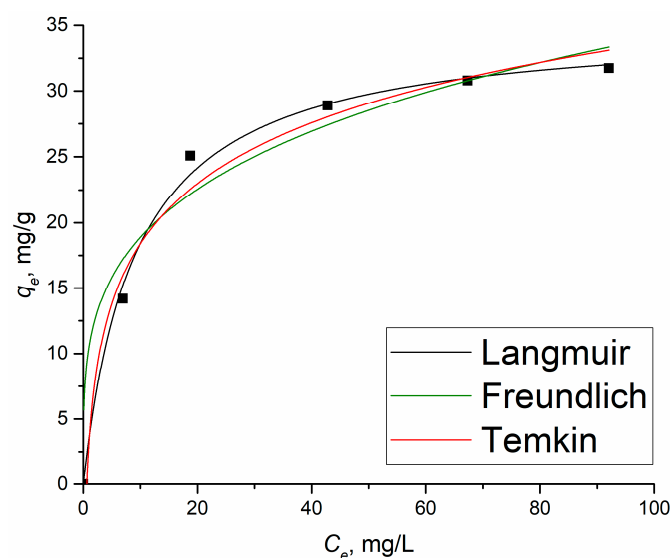


Figure 6. Plots of non-linear isotherm models for the adsorption of 2,4-D on Al₂O₃-0.25GO. Points are experimental data, lines are the fitting.

Comparing the obtained R² values of the applied models, the Langmuir and Freundlich equations describe the experimental data the best. This indicates that during the adsorption of 2,4-D, both chemical and physical interaction processes occur between the

adsorbate and the adsorbent [35]. It is clear that the Langmuir isotherm fits the isotherm data best, with the highest R^2 value of 0.996. Thus, based on the data presented in Table 2, it can be concluded that the adsorption of 2,4-D on the Al_2O_3 -GO sample followed the Langmuir isotherm and was monolayered.

Table 2. Isotherm parameters for 2,4-D.

Model Parameters		Calculated Values
Langmuir	q_m , mg/g	35.181
	b_l , L/g	0.109
	R^2	0.996
Freundlich	K_F , L/g	10.467
	$1/n$	0.256
	R^2	0.891
Temkin	b_T , J/mol	373.848
	A , L/g	1.601
	R^2	0.984

Table 3 shows comparative data on adsorption capacity, specific surface area and time to establish the adsorption equilibrium with respect to 2,4-D for different sorbents described in the literature. It shows that the suggested Al_2O_3 -0.25GO composite demonstrates a satisfactory adsorption capacity for the target component.

Table 3. Comparison of capacity values for 2,4-D ions absorbed by different adsorbents.

Adsorbent	q_e , mg/g	Equilibrium Time, Min	Ref.
[Co–Al–Cl] layered double hydroxide	20.51	60	[36]
Glutaraldehyde-crosslinked chitosan	252.55	-	[37]
Reduced graphene oxide	270.1	1440	[38]
Modified tiger-nut residue	90.2	120	[39]
Organophilic clay	6.45	6	[40]
Al_2O_3 -0.25GO	35.18	250	This work

4. Conclusions

In the present study, graphene oxide alumina granules were shown to have good adsorption capacity towards the pollutant herbicide 2,4-D. Experimental adsorption data were consistent with the Langmuir isotherm and the PSO model. Solution pH played a key role in adsorption efficiency, which may imply the predominance of electrostatic interactions in the adsorption process. 2,4-D was adsorbed most effectively at pH 2 to 4. However, adsorption was also observed at higher pH values, which may indicate that several mechanisms are involved in adsorption, such as, for example, π - π stacking or hydrogen bonds.

Author Contributions: Conceptualization, A.Y.K. and E.K.; methodology, A.Y.K. and E.K.; software, A.Y.K. and E.K.; validation, A.Y.K., E.K. and M.D.V.; formal analysis, A.Y.K., N.W.S.P. and E.K.; investigation, A.Y.K., E.K. and M.D.V.; resources, A.S., S.N.G. and M.D.V.; data curation, A.S., S.N.G. and M.D.V.; writing—original draft preparation, A.Y.K., E.K. and P.P.; writing—review and editing, A.Y.K., E.K. and P.P.; visualization, A.Y.K. and E.K.; supervision, A.S., S.N.G. and M.D.V.; project administration, A.S. and E.K.; funding acquisition, A.S. All authors have read and agreed to the published version of the manuscript.

Funding: This work was supported by the Ministry of Science and Higher Education of the Russian Federation under project 0707–2020–0034.

Data Availability Statement: Data are contained within the article.

Acknowledgments: The experiments were carried out using the equipment of the Centre of collective use of MSUT “STANKIN” (project No. 075-15-2021-695).

Conflicts of Interest: The authors declare no conflicts of interest.

References

1. Magnoli, K.; Carranza, C.S.; Aluffi, M.E.; Magnoli, C.E.; Barberis, C.L. Herbicides based on 2,4-D: Its behavior in agricultural environments and microbial biodegradation aspects. A review. *Environ. Sci. Pollut. Res.* **2020**, *27*, 38501–38512. [[CrossRef](#)]
2. Loomis, D.; Guyton, K.; Grosse, Y.; Ghissasi, F.E.; Bouvard, V.; Benbrahim-Tallaa, L.; Guha, N.; Mattock, H.; Straif, K. Carcinogenicity of lindane, DDT, and 2,4-dichlorophenoxyacetic acid. *Lancet Oncol.* **2015**, *16*, 891–892. [[CrossRef](#)] [[PubMed](#)]
3. Silva, A.P.; Morais, E.R.; Oliveira, E.C.; Ghisi, N.C. Does exposure to environmental 2,4-dichlorophenoxyacetic acid concentrations increase mortality rate in animals? A meta-analytic review. *Environ. Pollut.* **2022**, *303*, 119179. [[CrossRef](#)] [[PubMed](#)]
4. Kim, S.J.; Gobi, K.V.; Tanaka, H.; Shoyama, Y.; Miura, N. A simple and versatile self-assembled monolayer based surface plasmon resonance immunosensor for highly sensitive detection of 2,4-D from natural water resources. *Sensors Actuat. B Chem.* **2008**, *130*, 281–289. [[CrossRef](#)]
5. Gholamnia, R.; Abtahi, M.; Saeedi, R.; Khaloo, S.S. Synthesis and characterization of a new magnetic adsorbent for removal of 4-nitrophenol: Application of response surface methodology. *Water Sci Technol.* **2019**, *80*, 1430–1442. [[CrossRef](#)] [[PubMed](#)]
6. Vedenyapina, M.D.; Kurmysheva, A.Y.; Kryazhev, Y.G.; Ershova, V.A. Magnetic Iron-Containing Carbon Materials as Sorbents for the Removal of Pollutants from Aquatic Media (A Review). *Solid Fuel Chem.* **2021**, *55*, 285–305. [[CrossRef](#)]
7. Kumari, V.; Singh, P.P.; Kaushal, S. Synthesis and applications of metal-organic frameworks and graphene-based composites: A review. *Polyhedron* **2022**, *214*, 115645. [[CrossRef](#)]
8. Şahin, S.; Emik, S. Fast and highly efficient removal of 2,4-D using amino-functionalized poly (glycidyl methacrylate) adsorbent: Optimization, equilibrium, kinetic and thermodynamic studies. *J. Molec. Liq.* **2018**, *260*, 195–202. [[CrossRef](#)]
9. Kurmysheva, A.Y.; Yanushevich, O.; Krikheli, N.; Kramar, O.; Vedenyapina, M.D.; Podrabinnik, P.; Solís Pinargote, N.W.; Smirnov, A.; Kuznetsova, E.; Malyavin, V.V.; et al. Adsorption Ability of Graphene Aerogel and Reduced Graphene Aerogel toward 2,4-D, Herbicide and Salicylic Acid. *Gels* **2023**, *9*, 680. [[CrossRef](#)]
10. Won, D.S.; Park, I.-S.; Park, M.; Sohn, Y.; Kim, B.-G.; Nahm, K.S.; Chung, K.-S.; Kim, P. Graphene oxide templated alumina nanosheet for the removal of As(V). *Curr. Appl. Phys.* **2014**, *14*, 1245–1250. [[CrossRef](#)]
11. Abyzov, A.M. Alumina Oxide and Alumina Ceramics (review). Part 1. Properties of Al₂O₃ and Commercial Production of Dispersed Al₂O₃. *Refract. Ind. Ceram.* **2019**, *60*, 24–32. [[CrossRef](#)]
12. Grigoriev, S.N.; Trusova, E.A.; Afzal, A.M.; Soe, T.N.; Kurmysheva, A.Y.; Kuznetsova, E.; Smirnov, A.; Solís Pinargote, N.W. Peculiarities of γ -Al₂O₃ Crystallization on the Surface of h-BN Particles. *Materials* **2022**, *15*, 8054. [[CrossRef](#)] [[PubMed](#)]
13. Kurmysheva, A.Y.; Vedenyapina, M.D.; Kulaishin, S.A.; Podrabinnik, P.; Pinargote, N.W.S.; Smirnov, A.; Metel, A.S.; Bartolomé, J.F.; Grigoriev, S.N. Adsorption Removal of Mo(VI) from an Aqueous Solution by Alumina with the Subsequent Regeneration of the Adsorbent. *Int. J. Mol. Sci.* **2023**, *24*, 8700. [[CrossRef](#)] [[PubMed](#)]
14. Jacukowicz-Sobala, I.; Ociński, D.; Kociołek-Balawejder, E. Iron and aluminium oxides containing industrial wastes as adsorbents of heavy metals: Application possibilities and limitations. *Waste Manag. Res.* **2015**, *33*, 612–629. [[CrossRef](#)]
15. Zotov, R.; Meshcheryakov, E.; Livanova, A.; Minakova, T.; Magaev, O.; Isupova, L.; Kurzina, I. Influence of the Composition, Structure, and Physical and Chemical Properties of Aluminium-Oxide-Based Sorbents on Water Adsorption Ability. *Materials* **2018**, *11*, 132. [[CrossRef](#)]
16. Liu, L.; Zhang, B.; Zhang, Y.; He, Y.; Huang, L.; Tan, S.; Cai, X. Simultaneous Removal of Cationic and Anionic Dyes from Environmental Water Using Montmorillonite-Pillared Graphene Oxide. *J. Chem. Eng. Data* **2015**, *60*, 1270–1278. [[CrossRef](#)]
17. Shen, Y.; Fang, Q.; Chen, B. Environmental Applications of Three-Dimensional Graphene-Based Macrostructures: Adsorption, Transformation, and Detection. *Environ. Sci. Technol.* **2015**, *49*, 67–84. [[CrossRef](#)]
18. Czech, B.; Nasri-Nasrabadi, B.; Krzyszczak, A.; Sadok, I.; Hojamberdiev, M.; Yadav, R.; Shirvanimoghaddam, K.; Naebe, M. Enhanced PFAS adsorption with N-doped porous carbon beads from oil-sand asphaltene. *J. Water Process Eng.* **2023**, *54*, 104058. [[CrossRef](#)]
19. Grigoriev, S.N.; Soe, T.N.; Malakhinsky, A.; Makhadilov, I.; Romanov, V.; Kuznetsova, E.; Smirnov, A.; Podrabinnik, P.; Khmyrov, R.; Solís Pinargote, N.W.; et al. Granulation of Silicon Nitride Powders by Spray Drying: A Review. *Materials* **2022**, *15*, 4999. [[CrossRef](#)]
20. Li, Y.; Liu, J.; Deng, J.; He, J.; Qin, Y.; Xing, Y.; Yin, F. Fabrication of graphene oxide reinforced plasma sprayed Al₂O₃ coatings. *Ceram. Int.* **2023**, *49*, 1667–1677. [[CrossRef](#)]
21. Kuśmierk, K.; Szala, M.; Świątkowski, A. Adsorption of 2,4-dichlorophenol and 2,4-dichlorophenoxyacetic acid from aqueous solutions on carbonaceous materials obtained by combustion synthesis. *J. Taiwan Inst. Chem. Eng.* **2016**, *63*, 371–378. [[CrossRef](#)]
22. Vryonis, O.; Andritsch, T.; Vaughan, A.S.; Lewin, P.L. An alternative synthesis route to graphene oxide: Influence of surface chemistry on charge transport in epoxy-based composites. *J. Mater. Sci.* **2019**, *54*, 8302–8318. [[CrossRef](#)]
23. Sharma, N.; Sharma, V.; Jain, Y.; Kumari, M.; Gupta, R.; Sharma, S.K.; Sachdev, K. Synthesis and Characterization of Graphene Oxide (GO) and Reduced Graphene Oxide (rGO) for Gas Sensing Application. *Macromol. Symp.* **2017**, *376*, 1–5. [[CrossRef](#)]

24. Grigoriev, S.; Smirnov, A.; Pinargote, N.W.S.; Yanushevich, O.; Kriheli, N.; Kramar, O.; Pristiniski, Y.; Peretyagin, P. Evaluation of Mechanical and Electrical Performance of Aging Resistance ZTA Composites Reinforced with Graphene Oxide Consolidated by SPS. *Materials* **2022**, *15*, 2419. [[CrossRef](#)] [[PubMed](#)]
25. Santhiya, D.; Subramanian, S.; Natarajan, K.A.; Malghan, S.G. Surface chemical studies on alumina suspensions using ammonium poly(methacrylate). *Coll. Surf. A: Physicochem. Eng. Asp.* **2000**, *164*, 143–154. [[CrossRef](#)]
26. Tucureanu, V.; Matei, A.; Avram, A.M. FTIR Spectroscopy for Carbon Family Study. *Crit. Rev. Anal. Chem.* **2016**, *46*, 502–520. [[CrossRef](#)] [[PubMed](#)]
27. Lagergren, S. About the theory of so-called adsorption of soluble substances. *Sven. Vetenskapsakad. Handlingar* **1898**, *24*, 1–39.
28. Ho, Y.S.; McKay, G. Pseudo-second order model for sorption processes. *Proc. Biochem.* **1999**, *34*, 451–465. [[CrossRef](#)]
29. Zeldowitsch, J. The catalytic oxidation of carbon monoxide on manganese dioxide. *Acta Physicochim. URSS* **1934**, *1*, 364–449.
30. Vieira, T.; Becegato, V.A.; Paulino, A.T. Equilibrium Isotherms, Kinetics, and Thermodynamics of the Adsorption of 2,4-Dichlorophenoxyacetic Acid to Chitosan-Based Hydrogels. *Water Air Soil Pollut.* **2021**, *232*, 60. [[CrossRef](#)]
31. Gupta, S.S.; Bhattacharyya, K.G. Kinetics of adsorption of metal ions on inorganic materials: A review. *Adv. Colloid Interf. Sci.* **2011**, *162*, 39–58. [[CrossRef](#)]
32. Langmuir, I. The constitution and fundamental properties of solids and liquids. PART I. SOLIDS. *J. Franklin. Inst.* **1916**, *184*, 102–105. [[CrossRef](#)]
33. Gamal, R.; Rizk, S.E.; El-Hefny, N.E. The adsorptive removal of Mo(VI) from aqueous solution by a synthetic magnetic chromium ferrite nanocomposite using a nonionic surfactant. *J. Alloys Comp.* **2021**, *853*, 157039. [[CrossRef](#)]
34. Srivastava, V.; Sharma, Y.C.; Sillanpää, M. Application of nano-magneso ferrite (n-MgFe₂O₄) for the removal of Co²⁺ ions from synthetic wastewater: Kinetic, equilibrium and thermodynamic studies. *Appl. Surf. Sci.* **2015**, *338*, 42–54. [[CrossRef](#)]
35. Boumaraf, R.; Khettaf, S.; Benmahdi, F.; Masmoudi, R.; Ferhati, A. Removal of 2,4-dichlorophenoxyacetic acid from aqueous solutions by nanofiltration and activated carbon. *Biomass Conv. Bioref.* **2022**. [[CrossRef](#)]
36. Calisto, J.S.; Pacheco, I.S.; Freitas, L.L.; Santana, L.K.; Fagundes, W.S.; Amaral, F.A.; Canobre, S.C. Adsorption kinetic and thermodynamic studies of the 2,4-dichlorophenoxyacetate (2,4-D) by the [Co–Al–Cl] layered double hydroxide. *Heliyon* **2019**, *5*, e02553. [[CrossRef](#)] [[PubMed](#)]
37. Li, Q.; Su, H.; Yang, Y.; Zhang, J.; Xia, C.; Guo, Z. Adsorption property and mechanism of glutaraldehyde-crosslinked chitosan for removal of 2,4-dichlorophenoxyacetic acid from water. *Environ. Sci. Water Res. Technol.* **2023**, *9*, 294–307. [[CrossRef](#)]
38. Kuśmierk, K.; Świątkowski, A.; Skrzypczyńska, K.; Dąbek, L. Adsorptive and Electrochemical Properties of Carbon Nanotubes, Activated Carbon, and Graphene Oxide with Relatively Similar Specific Surface Area. *Materials* **2021**, *14*, 496. [[CrossRef](#)]
39. Kani, A.N.; Dovi, E.; Aryee, A.A.; Han, R.; Qu, L. Efficient removal of 2, 4-D from solution using a novel antibacterial adsorbent based on tiger nut residues: Adsorption and antibacterial study. *Environ. Sci. Pollut. Res.* **2022**, *29*, 64177–64191. [[CrossRef](#)]
40. Manzotti, F.; Santos, O.A.A. Evaluation of removal and adsorption of different herbicides on commercial organophilic clay. *Chem. Eng. Commun.* **2019**, *206*, 1515–1532. [[CrossRef](#)]

Disclaimer/Publisher’s Note: The statements, opinions and data contained in all publications are solely those of the individual author(s) and contributor(s) and not of MDPI and/or the editor(s). MDPI and/or the editor(s) disclaim responsibility for any injury to people or property resulting from any ideas, methods, instructions or products referred to in the content.